

Article

Millimetre Observations of Maser-Emitting Planetary Nebulae

Lucero Uscanga ^{1,*}, José R. Rizzo ², Miguel Santander-García ³, José F. Gómez ⁴, Luis F. Miranda ⁴, Olga Suárez ⁵, Panayotis Boumis ⁶, Mónica I. Rodríguez ⁷, Gerardo Ramos-Larios ⁸ and Roldán A. Cala ⁴

- ¹ Departamento de Astronomía, Universidad de Guanajuato, A.P. 144, Guanajuato 36000, Guanajuato, Mexico
- ² Centro de Astrobiología (INTA-CSIC), Ctra. M-108, km. 4, Torrejón de Ardoz, E-28850 Madrid, Spain; ricardo.rizzo@cab.inta-csic.es
- ³ Observatorio Astronómico Nacional (OAN-IGN), Alfonso XII, 3, E-28014 Madrid, Spain; m.santander@oan.es
- ⁴ Instituto de Astrofísica de Andalucía (CSIC), Glorieta de la Astronomía s/n, E-18008 Granada, Spain; jfg@iaa.es (J.F.G.); lfm@iaa.es (L.F.M.); rcala@iaa.es (R.A.C.)
- ⁵ Laboratoire Lagrange, Observatoire de la Côte d'Azur, Université Côte d'Azur, CNRS, Bd de l'Observatoire, CEDEX 4, 06304 Nice, France; olga.suarez@oca.eu
- ⁶ Institute for Astronomy, Astrophysics, Space Applications and Remote Sensing, National Observatory of Athens, 15236 Athens, Greece; ptb@astro.noa.gr
- ⁷ Instituto de Radioastronomía Milimétrica (IRAM), Av. Divina Pastora 7, E-18012 Granada, Spain; mrodriguez@iram.es
- ⁸ Instituto de Astronomía y Meteorología, Centro Universitario de Ciencias Exactas e Ingenierías (CUCEI), Universidad de Guadalajara, Av. Vallarta 2602, Arcos Vallarta, Guadalajara 44130, Jalisco, Mexico; gerardo@astro.iam.udg.mx
- * Correspondence: l.uscanga@ugto.mx

Abstract: Observations in the millimetre bands of maser-emitting planetary nebulae (PNe) are crucial to study their circumstellar molecular gas at the beginning of the PN phase. Maser-emitting PNe are in the earliest phases of PN formation; therefore, these sources are key objects to study the molecular content during the early evolution of PNe. These circumstellar envelopes are active sites for the formation of molecules. We present preliminary results of millimetre observations with the IRAM 30 m telescope towards one PN (IRAS 17393–2727) of a sample of five maser-emitting PNe, where we detect ¹²CO and ¹³CO lines in both $J = 1 \rightarrow 0$ and $J = 2 \rightarrow 1$ transitions.

Keywords: masers; planetary nebulae: general; stars: AGB and post-AGB; molecules



Citation: Uscanga, L.; Rizzo, J.R.; Santander-García, M.; Gómez, J.F.; Miranda, L.F.; Suárez, O.; Boumis, P.; Rodríguez, M.I.; Ramos-Larios, G.; Cala, R.A. Millimetre Observations of Maser-Emitting Planetary Nebulae. *Galaxies* **2022**, *10*, 48. <https://doi.org/10.3390/galaxies10020048>

Academic Editors: Martín Guerrero, Noam Soker and Quentin A. Parker

Received: 7 February 2022

Accepted: 8 March 2022

Published: 11 March 2022

Publisher's Note: MDPI stays neutral with regard to jurisdictional claims in published maps and institutional affiliations.



Copyright: © 2022 by the authors. Licensee MDPI, Basel, Switzerland. This article is an open access article distributed under the terms and conditions of the Creative Commons Attribution (CC BY) license (<https://creativecommons.org/licenses/by/4.0/>).

1. Introduction

Planetary nebulae (PNe) are one of the last phases in the evolution of low- and intermediate-mass stars ($\leq 8 M_{\odot}$). Their immediate precursors are stars in the asymptotic giant branch (AGB), followed by a short (≈ 100 – $10,000$ yr) transitional post-AGB phase.

The circumstellar envelopes of O-rich evolved stars provide optimal conditions to pump different species of masers. During the AGB phase, maser emission from the following molecules has been detected: SiO, H₂O, and OH [1]. Masers are potentially important tools in the study of PNe formation due to their short life times in evolved objects. For example: SiO, H₂O, and OH masers are expected to disappear ≈ 10 , 100, and 1000 yr, respectively, after the end of the AGB mass-loss [2,3]. Considering that the post-AGB phase is short, PNe showing H₂O and OH maser emissions are expected to be very young. Very few members of these special types of H₂O- and/or OH-emitting-PNe are known, including K3-35, IRAS 17347–3139, IRAS 18061–2505, IRAS 16333–4807, IRAS 15103–5754, JaSt 23, IRAS 17393–2727, IRAS 19219+0947 [4–11]

Thus, H₂O- and OH-emitting PNe could be among the youngest PNe, and therefore, they are key objects in the study of circumstellar molecular gas in very recently formed PNe.

The post-main sequence envelopes are very active sites for the production of molecules [12]. For example, HCN and HCO⁺ were detected in 13 of the 17 PNe with an

age range from 800 to 13,000 yr, at least in one transition [13]. Nine of them were common to both molecules. Later, [14] detected HNC in the same sample of PNe. In a recent molecular line survey in PNe, CN emission was common in most of the sources together with the molecules mentioned above [15]. Moreover, a robust dependence of the HNC/HCN line ratio on the UV luminosity of the PN central star was found. Furthermore, a marginal correlation between the HNC/HCN line ratio and PN age was identified [15].

The survival of molecules in the shells of PNe has been a subject of theoretical debate. Earlier models by [16] suggested that dusty cometary-like globules could shield molecular material and preserve it through the evolution of proto-PNe into PNe. Regarding maser-emitting PNe, K3-35 was the only source of this group where both HCO⁺ and ¹²CO had been detected until 2018 [17,18]. Now we know that IRAS 15103–5754 also harbours HCO⁺, C¹⁸O, and ¹²CO, that was mapped with ALMA [19].

2. Observations

We carried out millimetre (mm) observations with the Institut de Radioastronomie Millimétrique (IRAM) 30 m telescope in August 2014 towards a sample of five maser-emitting PNe. We used the Eight MIXer Receiver (EMIR) for all the observations. We selected simultaneous observations of ¹²CO $J = 1 \rightarrow 0$ (115.271 GHz), $J = 2 \rightarrow 1$ (230.538 GHz), and ¹³CO $J = 1 \rightarrow 0$ (110.201 GHz), and $J = 2 \rightarrow 1$ (220.399 GHz). The frequency resolution was ~ 200 kHz, corresponding to a velocity resolution of 0.5 km s^{-1} and 0.25 km s^{-1} at 3 mm and 1 mm, respectively. The bandwidth was 4 GHz. The *rms* (one-sigma) noise was between 5 mK and 92 mK at 3 mm and between 17 mK and 130 mK at 1 mm.

In order to associate the ¹²CO and ¹³CO line emission with the PN, we performed observations towards the source position and four off-source positions located 24 arcsec away from it, in the N, S, E and W directions. These 24 arcsec correspond to the half-power beam width (HPBW) at 3 mm, and twice the HPBW at 1 mm. This observational strategy was used previously by [20] while observing these molecular lines towards a particular type of post-AGB star known as water fountains (WFs).

3. Analysis

Data reduction and analysis were performed using the GILDAS software¹. We used the shell method available in GILDAS to fit the observed ¹²CO and ¹³CO lines in our sample. This method fits horn-type profiles for circumstellar envelopes and provides as outputs the parameters listed in Table 1 for the PN IRAS 17393–2727. In particular, we obtained the velocity of the emission peak (V_{pk}) at the centre of the line profile and the expansion velocity (V_{exp}) deduced from the full width at zero level.

Moreover, we used the code *shapemo1* that is included in the software SHAPE [21,22] to estimate some physical parameters of the molecular emission associated with this source. *shapemo1* produces synthetic spectral profiles of ¹²CO and ¹³CO lines to be compared with mm-range observations. See the next section for more details.

Table 1. Parameters of the ¹²CO and ¹³CO line emission in IRAS 17393–2727.

Line	V_{pk} (km s^{-1})	V_{exp} (km s^{-1})
¹² CO (1 \rightarrow 0)	−105.5 (1.0)	18.9 (1.4)
¹² CO (2 \rightarrow 1)	−106.0 (1.5)	17.5 (1.5)
¹³ CO (1 \rightarrow 0)	−106.9 (0.5)	15.4 (0.7)
¹³ CO (2 \rightarrow 1)	−107.0 (1.0)	16.2 (0.3)

Note. One-sigma errors within parentheses.

4. First Results

Circumstellar ¹²CO and ¹³CO line emission has been detected towards four of five sources in the sample (Uscanga et al., in prep). The emission from these molecules is only

present in the on-source position and not in the other four off-source positions (N, S, E, and W).

Here we present our first results in one PN, IRAS 17393–2727. The line emission is broad, with a width of $\sim 35 \text{ km s}^{-1}$ in the four lines observed (see Figure 1). All the intensities are given in a scale of main-beam temperature (T_{MB}), assuming main-beam efficiencies of 0.78 and 0.59 at 3 mm and 1 mm, respectively. Velocities are given with respect to the kinematic definition of the Local Standard of Rest (LSR). The intensities of the $J = 1 \rightarrow 0$ and $2 \rightarrow 1$ transitions of ^{12}CO emission in our spectra are similar to those reported by [23], also observed with the IRAM 30 m telescope, although our observations have a better signal-to-noise ratio, and we detected for the first time the $^{13}\text{CO } J = 1 \rightarrow 0$ and $2 \rightarrow 1$ transitions in this source (Uscanga et al., in prep).

The emission of ^{12}CO and ^{13}CO lines is located within the velocity range defined by the OH maser features at 1612 MHz with a velocity dispersion of $\sim 34 \text{ km s}^{-1}$ [24]. The average velocity of the emission peak of the four emission lines (weighted by the inverse square of the errors) is $\simeq -106.6 \pm 0.4 \text{ km s}^{-1}$ (Table 1). We used this value as the systemic velocity for the model of the molecular envelope of the PN IRAS 17393–2727 and compared the synthetic spectra, generated with `shapemo1`, against the observed ones (Figure 1).

There is only one estimation for the distance to this source $\sim 1.2 \text{ kpc}$, based on statistical methods [25]. The kinematic distance is $\sim 8 \text{ kpc}$. There is no counterpart to this source, neither in Gaia DR2 nor in Gaia Early DR3; the closest source does not have a measured parallax [26,27]. We build models for three different distances: the statistical one ($\sim 1.2 \text{ kpc}$), the kinematic one ($\sim 8 \text{ kpc}$), and an intermediate value ($\sim 5 \text{ kpc}$). We obtained a molecular mass range from $0.007 M_{\odot}$ at 1.2 kpc to $0.6 M_{\odot}$ at 8 kpc. However, the best-fit model for the emission in ^{12}CO and ^{13}CO is at 5 kpc with the physical parameters listed in Table 2.

Given the scarcity of information on the spatial distribution of ^{12}CO and ^{13}CO line emission, with only an on-source pointing and four off-source positions, we resorted to a model as geometrically simple as possible, that is, a filled sphere with a radius of $4.5 \times 10^{17} \text{ cm}$, a typical size for AGB envelopes, with constant values for density and temperature. The only spatial dependence of the model is that on the expansion velocity, for which we considered a linear dependence on radius similar to that found in many young PNe, a homologous expansion. The maximum value of the velocity was 19 km s^{-1} (see Table 2). This is consistent with the average expansion velocity of the envelope obtained from the four emission lines (weighted by the inverse square of the errors) of $\sim 16.2 \pm 0.3 \text{ km s}^{-1}$ (Table 1).

Table 2. Best-fit model physical parameters for the molecular emission of IRAS 17393–2727.

Parameter	Value
Assumed Distance	5 kpc
Envelope Radius	$4.5 \times 10^{17} \text{ cm}$
Systemic Velocity (V_{LSR})	-106.6 km s^{-1}
Expansion Velocity, Linear Pattern, V_{max}	19 km s^{-1}
Microturbulence Velocity (δ_V)	2 km s^{-1}
Temperature (T)	190 K
Molecular Mass	$0.28 M_{\odot}$
Total Density (n)	$3.1 \times 10^2 \text{ cm}^{-3}$
$X(^{12}\text{CO})$	9.0×10^{-5}
$X(^{13}\text{CO})$	1.7×10^{-5}

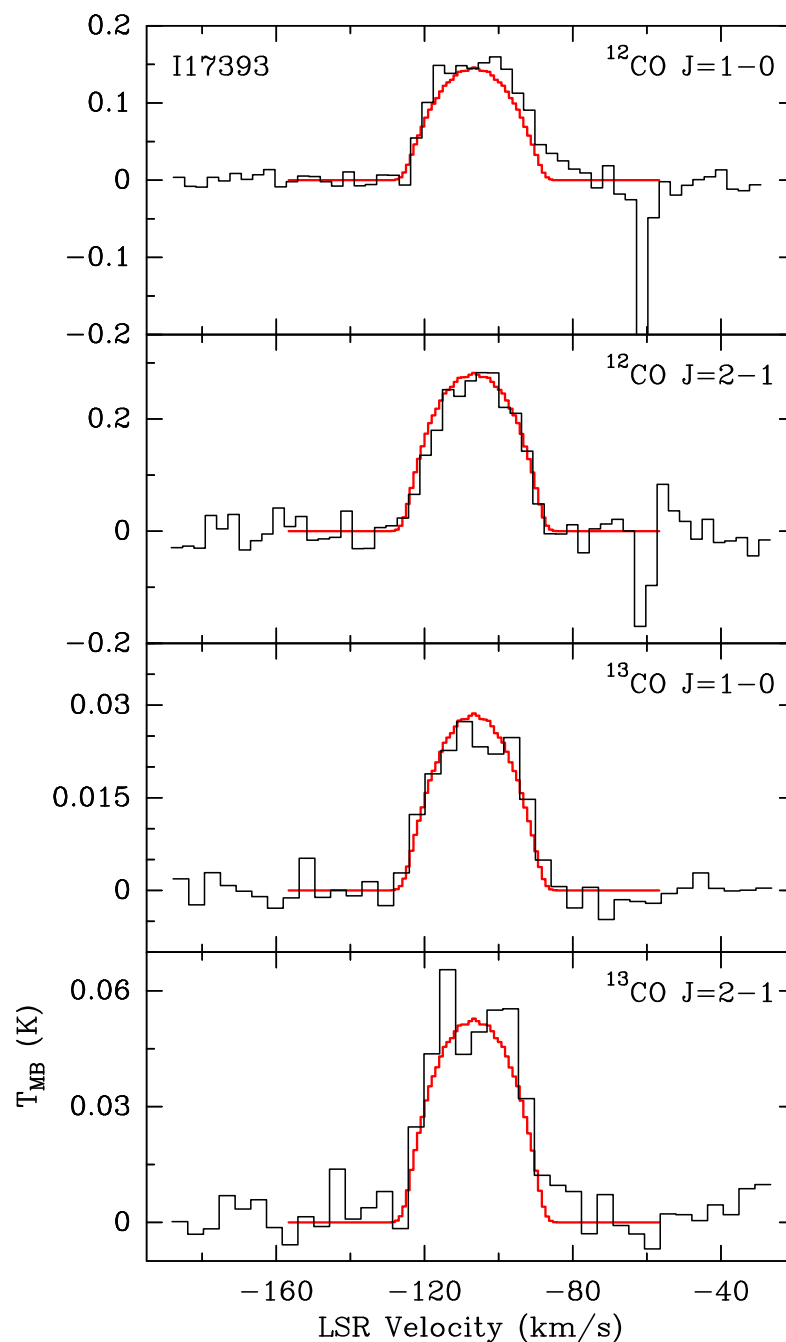


Figure 1. Synthetic spectra (red) and observations (black) for ^{12}CO and ^{13}CO transitions detected in IRAS 17393–2727 with the IRAM 30 m telescope. The (shortened) source name is indicated at the top of the first panel. Note the different intensity ranges in the panels. All the spectra span 175 km s^{-1} of coverage. The original spectra have been smoothed at a velocity resolution of 3 km s^{-1} .

5. Discussion and Future Work

In the model, the total size of the envelope at the assumed distance is ~ 12 arcsec. This is about the size of the HPBW at 1 mm in our observations. In addition, an HST image of IRAS 17393–2727 shows a collimated, bipolar outflow of ~ 2.2 arcsec in extent, with the two parts of the outflow separated by a dark region of ~ 0.6 arcsec. Therefore, the assumed molecular envelope has a larger size than the outflow observed at optical wavelengths.

We have found a molecular mass of $0.28 M_{\odot}$ for IRAS 17393–2727. This value is quite similar to the masses reported in other maser-emitting evolved objects, i.e., WFs [20]. These sources are in a previous evolutionary stage, the post-AGB phase. They present high-velocity jets traced by H_2O maser emission [28].

The abundance X of the species ^{12}CO and ^{13}CO is listed at the end of Table 2. The $^{12}\text{CO}/^{13}\text{CO}$ ratio is ~ 5.3 , which is quite similar to other PNe (especially O-rich) such as NGC 6302 [22,29]. However, another C-rich nebula, NGC 7027, may reach a $^{12}\text{CO}/^{13}\text{CO}$ ratio ~ 50 [30] even though it is a young PN. On the other hand, O-rich AGB stars present $^{12}\text{C}/^{13}\text{C}$ ratios $\sim 10\text{--}35$ [31], while in post-AGB stars such as WFs, this ratio is $\sim 7\text{--}30$ [20]. We are still working in the analysis of the abundances of IRAS 17393–2727 and the other sources of our sample to reach a conclusive result, keeping in mind the uncertainties of these estimations.

For future work, we plan to study the molecular content of very young PNe, especially PNe with maser emission, and determine the physical parameters of the molecular gas, namely v , T , M , n . We will also measure the fractional abundances of HCN and HCO^+ and compare them with the values obtained in more evolved PNe. Finally, we will carry out high-resolution observations of these sources to define the structures associated with these molecular emissions (envelope, torus, and outflow).

Author Contributions: Conceptualization, L.U., J.F.G., J.R.R., L.F.M., O.S. and P.B.; methodology, L.U., J.R.R. and J.F.G.; software, J.R.R. and M.S.-G.; formal analysis, L.U., J.R.R. and M.S.-G.; investigation, L.U.; data curation, L.U., J.R.R., M.S.-G. and M.I.R.; writing—original draft preparation, L.U.; writing—review and editing, L.U., J.R.R., M.S.-G., J.F.G., L.F.M., M.I.R., G.R.-L. and R.A.C.; visualization, L.U.; supervision, L.U.; project administration, L.U.; funding acquisition, L.U. All authors have read and agreed to the published version of the manuscript.

Funding: L.U. acknowledges support from the University of Guanajuato (Mexico) grant ID CIIC 164/2022.

Acknowledgments: We would like to thank the telescope operator and staff of the 30 m IRAM radio telescope for their assistance. L.U. is grateful with the undergraduate students L.C. Cabal-Paramo and S.J. González-Enriquez for gathering the references information.

Conflicts of Interest: The authors declare no conflict of interest.

Notes

- ¹ GILDAS is a radio astronomy software developed by IRAM. See <http://www.iram.fr/IRAMFR/GILDAS/> (accessed on 7 March 2022).

References

1. Reid, M.J.; Moran, J.M. Masers. *Annu. Rev. Astron. Astrophys.* **1981**, *19*, 231–276. [[CrossRef](#)]
2. Lewis, B.M. Kinematics and Chemical Properties of the Old Disk in the Galaxy. *Astrophys. J.* **1989**, *338*, 234. [[CrossRef](#)]
3. Gómez, Y.; Moran, J.M.; Rodríguez, L.F. H_2O and SiO maser emission in OH/IR stars. *Rev. Mex. Astron. Astrofis.* **1990**, *20*, 55.
4. Miranda, L.F.; Gómez, Y.; Anglada, G.; Torrelles, J.M. Water-maser emission from a planetary nebula with a magnetized torus. *Nature* **2001**, *414*, 284–286. [[CrossRef](#)] [[PubMed](#)]
5. de Gregorio-Monsalvo, I.; Gómez, Y.; Anglada, G.; Cesaroni, R.; Miranda, L.F.; Gómez, J.F.; Torrelles, J.M. A Survey for Water Maser Emission toward Planetary Nebulae: New Detection in IRAS 17347–3139. *Astrophys. J.* **2004**, *601*, 921–929. [[CrossRef](#)]
6. Tafoya, D.; Gómez, Y.; Patel, N.A.; Torrelles, J.M.; Gómez, J.F.; Anglada, G.; Miranda, L.F.; de Gregorio-Monsalvo, I. A Collimated, Ionized Bipolar Structure and a High Density Torus in the Planetary Nebula IRAS 17347–3139. *Astrophys. J.* **2009**, *691*, 611–620. [[CrossRef](#)]
7. Gómez, J.F.; Suárez, O.; Gómez, Y.; Miranda, L.F.; Torrelles, J.M.; Anglada, G.; Morata, O. Radio Interferometric Observations of Candidate Water-Maser-Emitting Planetary Nebulae. *Astron. J.* **2008**, *135*, 2074–2083. [[CrossRef](#)]
8. Uscanga, L.; Gómez, J.F.; Miranda, L.F.; Boumis, P.; Suárez, O.; Torrelles, J.M.; Anglada, G.; Tafoya, D. H_2O maser emission associated with the planetary nebula IRAS 16333–4807. *Mon. Not. R. Astron. Soc.* **2014**, *444*, 217–221. [[CrossRef](#)]
9. Qiao, H.-H.; Walsh, A.J.; Gómez, J.F.; Imai, H.; Green, J.A.; Dawson, J.R.; Shen, Z.-Q.; Ellingsen, S.P.; Breen, S.L.; Jones, P.A.; et al. Unusual Shock-excited OH Maser Emission in a Young Planetary Nebula. *Astrophys. J.* **2016**, *817*, 37. [[CrossRef](#)]
10. Gómez, J.F.; Suárez, O.; Bendjoya, P.; Rizzo, J.R.; Miranda, L.F.; Green, J.A.; Uscanga, L.; García-García, E.; Lagadec, E.; Guerrero, M.A.; et al. The First Water Fountain in a Planetary Nebula with Synchrotron Emission. *Astrophys. J.* **2015**, *799*, 186. [[CrossRef](#)]
11. Uscanga, L.; Gómez, J.F.; Suárez, O.; Miranda, L.F. An updated catalog of OH-maser-emitting planetary nebulae. *Astron. Astrophys.* **2012**, *547*, A40. [[CrossRef](#)]
12. Zhang, Y. Planetary Nebulae: Multi-Wavelength Probes of Stellar and Galactic Evolution. In Proceedings of the IAU Symposium No. 323: Planetary Nebulae: Multi-Wavelength Probes of Stellar and Galactic Evolution, Beijing, China, 10–14 October 2016; Liu, X., Stanghellini, L., Karakas, A., Eds.; Cambridge University Press: Cambridge, UK, 2017; Volume 323, p. 141.

13. Schmidt, D.R.; Ziurys, L.M. Hidden Molecules in Planetary Nebulae: New Detections of HCN and HCO⁺ from a Multi-object Survey. *Astrophys. J.* **2016**, *817*, 175. [[CrossRef](#)]
14. Schmidt, D.R.; Ziurys, L.M. New Detections of HNC in Planetary Nebulae: Evolution of the [HCN]/[HNC] Ratio. *Astrophys. J.* **2017**, *835*, 79. [[CrossRef](#)]
15. Bublitz, J.; Kastner, J.H.; Santander-García, M.; Bujarrabal, V.; Alcolea, J.; Montez, R. A new radio molecular line survey of planetary nebulae. HNC/HCN as a diagnostic of ultraviolet irradiation. *Astron. Astrophys.* **2019**, *625*, A101. [[CrossRef](#)]
16. Howe, D.A.; Hartquist, T.W.; Williams, D.A. Molecules in dense globules in planetary nebulae. *Mon. Not. R. Astron. Soc.* **1994**, *271*, 811–816. [[CrossRef](#)]
17. Tafoya, D.; Gómez, Y.; Anglada, G.; Loinard, L.; Torrelles, J.M.; Miranda, L.F.; Osorio, M.; Franco-Hernández, R.; Nyman, L.-A.; Nakashima, J.; et al. Detection of HCO⁺ Emission toward the Planetary Nebula K3–35. *Astron. J.* **2007**, *133*, 364–369. [[CrossRef](#)]
18. Sánchez-Contreras, C.; Sahai, R. OPACOS: OVRO Post-AGB CO(1–0) Emission Survey. I. Data and Derived Nebular Parameters. *Astrophys. J. Suppl. Ser.* **2012**, *203*, 16. [[CrossRef](#)]
19. Gómez, J.F.; Niccolini, G.; Suárez, O.; Miranda, L.F.; Rizzo, J.R.; Uscanga, L.; Green, J.A.; de Gregorio-Monsalvo, I. ALMA imaging of the nascent planetary nebula IRAS 15103–5754. *Mon. Not. R. Astron. Soc.* **2018**, *480*, 4991–5009. [[CrossRef](#)]
20. Rizzo, J.R.; Gómez, J.F.; Miranda, L.F.; Osorio, M.; Suárez, O.; Durán-Rojas, M.C. Sensitive CO and ¹³CO survey of water fountain stars. Detections towards IRAS 18460–0151 and IRAS 18596+0315. *Astron. Astrophys.* **2013**, *560*, A82. [[CrossRef](#)]
21. Steffen, W.; Koning, N.; Wenger, S.; Morisset, C.; Magnor, M. Shape: A 3D modeling tool for astrophysics. *IEEE Trans. Vis. Comput. Graph.* **2011**, *17*, 454–465. [[CrossRef](#)]
22. Santander-García, M.; Bujarrabal, V.; Koning, N.; Steffen, W. SHAPEMOL: A 3D code for calculating CO line emission in planetary and protoplanetary nebulae. Detailed model-fitting of the complex nebula NGC 6302. *Astron. Astrophys.* **2015**, *573*, A56. [[CrossRef](#)]
23. Mauersberger, R.; Henkel, C.; Wilson, T.L.; Olano, C.A. The detection of CO in a proto-planetary nebula close to the galactic center. *Astron. Astrophys.* **1988**, *206*, L34–L36.
24. Gómez, J.F.; Uscanga, L.; Green, J.A.; Miranda, L.F.; Suárez, O.; Bendjoya, P. Polarization properties of OH emission in planetary nebulae. *Mon. Not. R. Astron. Soc.* **2016**, *461*, 3259–3273. [[CrossRef](#)]
25. Preite-Martinez, A. Possible new planetary nebulae in the IRAS point source catalogue. *Astrophys. J. Suppl. Ser.* **1988**, *76*, 317–330.
26. Collaboration, G. Gaia Data Release 2. Summary of the contents and survey properties. *Astron. Astrophys.* **2018**, *616*, A1. [[CrossRef](#)]
27. Collaboration, G. Gaia Early Data Release 3. Summary of the contents and survey properties. *Astron. Astrophys.* **2021**, *649*, A1. [[CrossRef](#)]
28. Imai, H. Stellar molecular jets traced by maser emission. In Proceedings of the IAU Symposium No. 242: Astrophysical Masers and Their Environments, Alice Springs, Australia, 12–16 March 2007; Chapman, J.M., Baan, W.A., Eds.; Cambridge University Press: Cambridge, UK, 2007; Volume 242, pp. 279–286.
29. Bujarrabal, V.; Alcolea, J.; Van Winckel, H.; Santander-García, M.; Castro-Carrizo, A. Extended rotating disks around post-AGB stars. *Astron. Astrophys.* **2013**, *557*, A104. [[CrossRef](#)]
30. Santander-García, M.; Bujarrabal, V.; Alcolea, J. Modeling the physical and excitation conditions of the molecular envelope of NGC 7027. *Astron. Astrophys.* **2012**, *545*, A114. [[CrossRef](#)]
31. Milam, S.N.; Woolf, N.J.; Ziurys, L.M. Circumstellar ¹²C/¹³C Isotope Ratios from Millimeter Observations of CN and CO: Mixing in Carbon- and Oxygen-Rich Stars. *Astrophys. J.* **2009**, *690*, 837. [[CrossRef](#)]